Loss of pVHL is sufficient to cause HIF dysregulation in primary cells but does not promote tumor growth

Fiona A. Mack,[1] W. Kimryn Rathmell,[1] Andrew M. Arsham,[1,2] James Gnarra,[3]
Brian Keith,[1] and M. Celeste Simon[1,2,*]

[1]Abramson Family Cancer Research Institute
[2]Howard Hughes Medical Institute
University of Pennsylvania School of Medicine, Philadelphia, Pennsylvania 19104
[3]Department of Biochemistry and Molecular Biology, Louisiana State University Medical Center, New Orleans, Louisiana 70112
*Correspondence: celeste2@mail.med.upenn.edu

Summary

Inactivation of the von Hippel-Lindau (*VHL*) gene is associated with the development of highly vascularized tumors. pVHL targets the α subunits of hypoxia inducible factor (HIF) for ubiquitin-mediated degradation in an oxygen-dependent manner. Although pVHL-deficient tumor cell lines demonstrate constitutive stabilization and activation of HIF, it has yet to be shown that loss of murine *Vhl* alone is sufficient to dysregulate HIF. We utilized a genetic approach to demonstrate that loss of *Vhl* is sufficient not only to stabilize HIF-α subunits under normoxia, but also fully activate HIF-mediated responses. These studies have implications for the hierarchy of signaling events leading to HIF stabilization, nuclear translocation, and target gene expression. We further demonstrate that loss of murine *Vhl* does not promote teratocarcinoma growth, indicating that other genetic changes must occur to facilitate *Vhl*-mediated tumorigenesis.

Introduction

von Hippel-Lindau disease is an autosomal dominant hereditary cancer syndrome. Patients heterozygous for one inactivating mutation within the von Hippel-Lindau (*VHL*) gene are predisposed to the development of pheochromocytomas and a variety of highly vascularized tumors, including renal clear cell carcinomas, retinal angiomas, and hemangioblastomas (Maher and Kaelin,, 1997). Within these tumors, the second *VHL* allele has been rendered inactive by deletions, mutations, or hypermethylation. *VHL* is therefore a classic tumor suppressor conforming to the Knudson two hit hypothesis in which the second inactivating mutation occurs within somatic cells. A majority of sporadic renal clear cell carcinomas also exhibit biallelic loss of *VHL* function, further supporting *VHL*'s role as a tumor suppressor (Foster et al., 1994; Gnarra et al., 1994). Animal models demonstrate that deletion of murine *Vhl* function results in lethality, as *Vhl*$^{-/-}$ mice die in utero between E10.5–E12 due to placental vascular abnormalities (Gnarra et al., 1997). Hepatocyte-specific loss of *Vhl* in adult mice results in the formation of hemangiomas within the liver, a phenotype rarely observed in human *VHL* patients (Haase et al., 2001).

pVHL, the protein product of the *VHL* gene, interacts through its α domain with elongins B/C and Cul2 to form the VBC complex, an E3 ubiquitin ligase. This multiprotein complex targets proteins for ubiquitin-mediated degradation, analogous to the *S. cerevisiae* SCF (Skp1/Cdc53/F-box) ubiquitination machinery (Pause et al., 1997; Lonergan et al., 1998; Lisztwan et al., 1999). Although pVHL has no sequence homology to any known proteins, it is functionally similar to the F box protein of SCF by binding specific substrates through its β domain (Ohh et al., 2000).

Major targets of the VBC complex include the regulatory α subunits of the heterodimeric transcription factor hypoxia inducible factor (HIF). HIF modulates both cellular and systemic responses to changes in oxygen (O_2) concentrations by stimulating the expression of genes involved in energy metabolism, angiogenesis, hematopoiesis, and O_2 delivery. Proteasome inhibitor studies show that at high levels of O_2 (21%), the VBC complex binds HIF-α subunits (HIF-1α and HIF-2α), targeting them for ubiquitination and degradation via the 26S proteasome (Maxwell et al., 1999). Low O_2 (hypoxia) disrupts the association of pVHL with HIF-α subunits, which then dimerize with constitutively expressed ARNT/HIF-β to form transcriptionally active HIF. Mutations within the β domain of pVHL disrupt its interaction with HIF-α subunits leading to constitutive HIF-α stabiliza-

SIGNIFICANCE

Loss of the pVHL tumor suppressor protein is associated with tumors within the CNS, retina, and kidney. pVHL targets the α subunits of hypoxia inducible factor (HIF) for ubiquitin-mediated degradation in an O_2-regulated manner. The degree to which constitutive HIF stabilization contributes to *VHL* disease has been studied in tumor-derived cell lines that contain other genetic lesions. We generated primary *Vhl*$^{-/-}$ ES cells that display maximal HIF activity under normoxic conditions. These results contrast published reports indicating that full HIF activity requires multiple pVHL-independent, O_2-regulated steps, including nuclear transport and transactivation. Surprisingly, *Vhl*$^{-/-}$ ES cells generate smaller teratocarcinomas than controls, suggesting a growth disadvantage in pVHL-deficient primary cells. Therefore, *VHL*'s tumor suppressor activity may be manifested only in a background of other mutations.

tion and HIF activity (Cockman et al., 2000; Ohh et al., 2000). Furthermore, *VHL*$^{-/-}$ renal clear cell carcinoma (RCC) cell lines fail to degrade HIF-α subunits under normoxic conditions. These cells display constitutive expression of HIF targets including genes encoding erythropoietin (EPO), vascular endothelial growth factor (VEGF), glucose transporter (GLUT-1), and phosphoglycerate kinase (PGK) (Iliopoulos et al., 1996; Maxwell et al., 1999; Krieg et al., 2000). In addition to its role as part of an E3 ubiquitin ligase, pVHL is required for proper fibronectin deposition, cytoskeletal reorganization, growth arrest upon serum withdrawal, and contact inhibition, although the underlying mechanisms for these properties remain unclear (Ohh et al., 1998; Pause et al., 1998; Hoffman et al., 2001; Kamada et al., 2001; Bindra et al., 2002). Defects within all of these pathways can be reversed by reintroduction of wild-type pVHL into *VHL*$^{-/-}$ RCC cells.

The interaction of pVHL with HIF-α is one of several O_2-dependent events thought to regulate HIF activity. First, pVHL binding to HIF-α subunits is dependent upon hydroxylation of key proline residues within the O_2-dependent degradation (ODD) domain of HIF-α (Ivan et al., 2001; Jaakkola et al., 2001). A recently defined family of HIF prolyl-hydroxylases (HIF-PHs) catalyzes this iron- and O_2-dependent reaction. All three elements of this pathway are conserved in *C. elegans, Drosophila*, and mammals (Bruick and McKnight 2001; Epstein et al., 2001). Second, hypoxia is also believed to induce the nuclear accumulation of stabilized HIF-α subunits, protecting them from pVHL-mediated degradation (Kallio et al., 1999; Tanimoto et al., 2000). Third, hypoxia-mediated HIF transactivation of target genes requires interactions with coactivators p300 and CBP (Arany et al., 1996; Jiang et al., 1997; Pugh et al., 1997; Ebert and Bunn, 1998; Carrero et al., 2000). Recent studies suggest that hydroxylation of a C-terminal activation domain (CAD) asparagine residue by an iron- and O_2-dependent asparagyl hydroxylase disrupts HIF-α binding to coactivators p300 and CBP, thereby preventing transactivation during normoxia (Lando et al., 2002). Furthermore, hydroxylation within the CAD is thought to occur in a pVHL-independent manner (Sang et al., 2002). Therefore, under normal O_2 concentrations, hydroxylation of HIF-α on proline and asparagine residues regulates HIF's transcriptional activity by targeting the protein for proteolysis and inhibiting binding to coactivators, respectively.

Thus far, most studies correlating loss of *VHL* function with HIF dysregulation have been conducted in renal tumors and fully transformed cell lines. As cancer development requires multiple genetic lesions, these cells undoubtedly contain a highly abnormal genetic background. Although recent results have shown that *VHL* inactivation is correlated with stimulation of the HIF pathway in early kidney lesions (Mandriota et al., 2002), other genetic abnormalities were not examined. Indeed, cytogenetic analysis of renal clear cell carcinomas shows that a majority of these tumors have lost the short arm of chromosome 3 and contain a myriad of structural aberrations and unbalanced translocations (Gunawan et al., 2001). Although reintroduction of *VHL* into RCC lines eliminates their tumorigenic phenotype (Gnarra et al., 1996; Iliopoulos et al., 1996), this occurs within a background of uncharacterized mutations, making it difficult to identify the effects of *VHL* loss alone. Until now, a formal genetic study to assess the tumorigenic effects of *VHL* loss in euploid primary cells has not been performed. Furthermore, although the regulation of HIF activity is believed to be a multistep process responsive to O_2 levels, it is unclear to what degree these events can occur in normoxic conditions. Here, we utilize gene targeting of *Vhl* in mouse embryonic stem (ES) cells to demonstrate that loss of *Vhl* is sufficient to dysregulate HIF degradation, nuclear accumulation, DNA binding activity, and downstream target gene activation, conferring a hypoxic phenotype to normoxic *Vhl*$^{-/-}$ ES cells. Unexpectedly, *Vhl*$^{-/-}$ teratocarcinomas are smaller by volume and mass compared to *Vhl*$^{+/-}$ tumors, suggesting that stimulation of the HIF pathway is not sufficient to induce tumor growth and additional genetic changes must occur to facilitate tumorigenesis in the absence of *Vhl*.

Results

Generation of *Vhl*$^{-/-}$ ES cells

Although renal cancer cell lines deficient for pVHL exhibit constitutive expression of HIF target genes under normoxic conditions, loss of *VHL* alone has not been shown to result in complete disruption of HIF regulation and promotion of tumor formation. To examine the precise role of *Vhl* in these processes, we utilized a genetic strategy based on *Vhl*$^{+/-}$ mouse J1 embryonic stem (ES) cells (Gnarra et al., 1997). The recombined locus maintains intact the *Vhl* promoter region, the first 23 codons, and 3′ untranslated region (Figure 1A). Homozygous *Vhl*$^{-/-}$ clones were generated from *Vhl*$^{+/-}$ ES cells by selecting for loss of the remaining wild-type allele with increasing concentrations of G418 (Mortensen et al., 1992). Approximately 200 clones were screened for loss of heterozygosity by Southern blot and/or PCR assays (Figures 1B and 1C). Three independently derived *Vhl*$^{-/-}$ clones were identified, none of which expressed detectable amounts of pVHL when compared to *Vhl*$^{+/+}$ and *Vhl*$^{+/-}$ ES cells (Figure 1D), and these were further assayed for HIF function.

HIF is constitutively stabilized and maintains DNA binding activity in the absence of *Vhl*

We first investigated the stabilization of HIF-α proteins by Western blot and electrophoretic mobility shift assay (EMSA). Immunoblots of nuclear extracts demonstrated that at 21% O_2 (normoxia) (Figure 2A), *Vhl*$^{+/+}$ and *Vhl*$^{+/-}$ ES cells express low levels of HIF-1α and HIF-2α, which increased dramatically at 1.5% O_2 (hypoxia). In contrast, *Vhl*$^{-/-}$ cells accumulated high levels of HIF-1α and HIF-2α under normoxia. Moreover, HIF-1α and HIF-2α protein levels remained largely unchanged within normoxic and hypoxic extracts when normalized to the Rad50 loading control. The constitutive stabilization of HIF-α subunits in *Vhl*$^{-/-}$ cells is consistent with data reported for RCC lines (Maxwell et al., 1999; Krieg et al., 2000).

The nuclear translocation of HIF-α subunits has been reported to be an O_2-regulated step, independent of pVHL function (Tanimoto et al., 2000). To detect the localization of constitutively stabilized HIF-1α in *Vhl*$^{-/-}$ cells, Western blots were performed using cytoplasmic and nuclear fractions of extracted proteins (Figure 2B). In *Vhl*$^{+/+}$ and *Vhl*$^{+/-}$ cells, stabilized HIF-1α was exclusively detected in the nuclear fraction of hypoxic extracts (Figure 2B). All *Vhl*$^{-/-}$ clones exhibited exclusively nuclear accumulation of HIF-1α under normoxia and hypoxia. Introduction of hemagglutin-tagged (HA)-VHL into clone *Vhl*$^{-/-.1}$ restored the hypoxic regulation of HIF-1α, consistent with previously reported data (Maxwell et al., 1999; Krieg et al., 2000). This

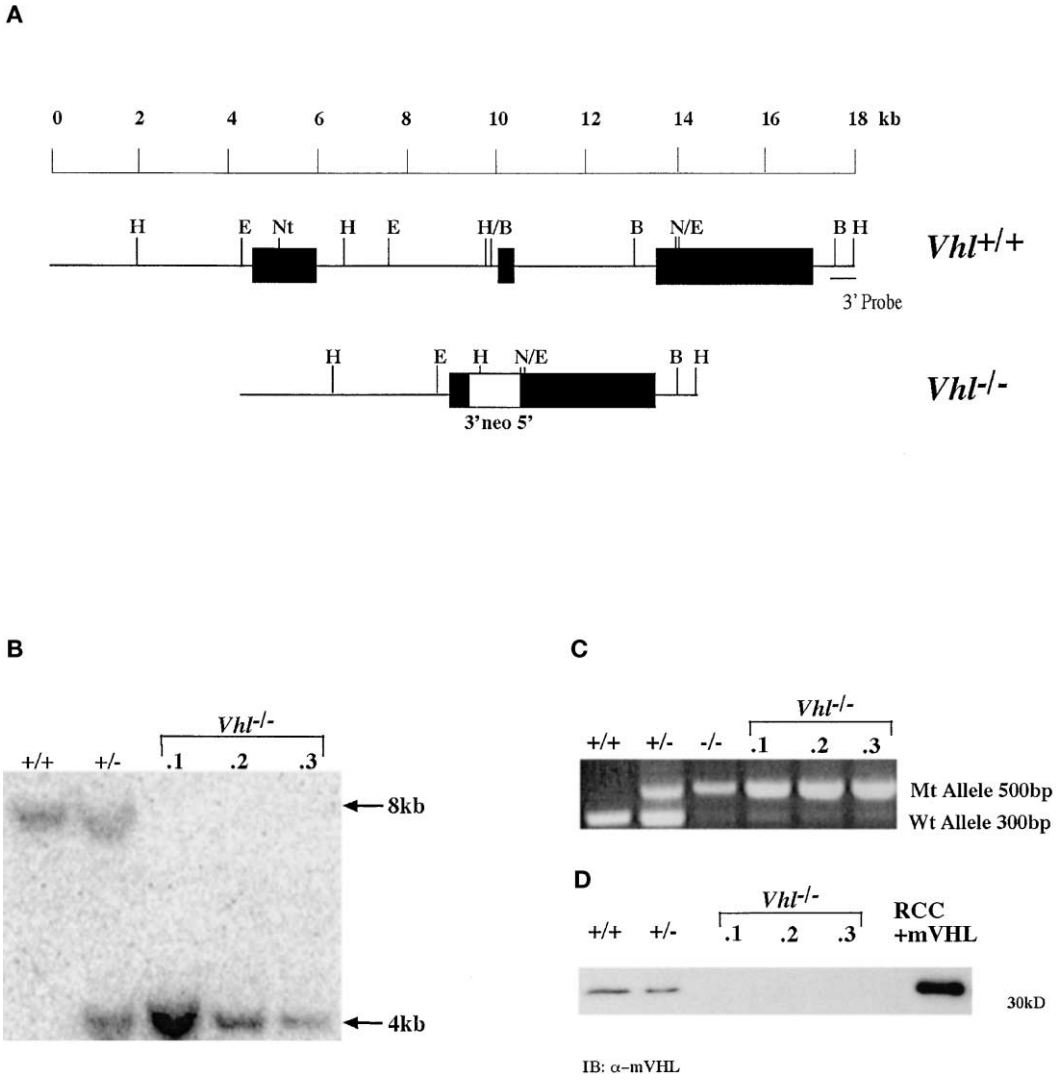

Figure 1. Generation of *Vhl*$^{-/-}$ ES cells

A: Filled boxes represent the three *Vhl* exons while the open box depicts the pgk-neo selectable marker within the targeting vector. The 3′ flanking probe used in Southern blots is indicated.

B: Detection of wild-type and targeted alleles in ES cells by HindIII digestion and hybridization to the 3′ flanking probe revealed an 8 kb wild-type fragment and a 4 kb mutant fragment in *Vhl*$^{+/-}$ and ES clones 1, 2, and 3.

C: PCR genotyping of ES clones demonstrated a 300 bp wild-type and a 500 bp mutant product. The lower band visible within lanes 3–6 is a background signal thought not to represent the wild-type allele because of its greater size and decreased intensity.

D: Immunoblot for pVHL in ES clones detected a 30 kDa protein in wild-type and *Vhl*$^{+/-}$ ES cell whole-cell extracts but not in clones 1, 2, and 3. A pVHL-deficient RCC cell line stably transfected with HA-tagged murine pVHL was used as a control.

"rescued" *Vhl*$^{-/-}$ clone expressed levels of pVHL comparable to RCC lines rescued with HA-VHL (data not shown) (Iliopoulos et al., 1996).

HIF DNA binding activity in normoxic and hypoxic *Vhl*$^{-/-}$ ES cells was assessed by EMSA. *Vhl*$^{+/-}$ ES cells exhibited hypoxic induction of a DNA complex confirmed to be HIF by "supershifting" with an α-ARNT antibody (Figure 2C, lanes 2 and 3). In contrast, high levels of HIF were detected in normoxic *Vhl*$^{-/-}$ ES cells (Figure 2C, lanes 4, 7, and 10), which was also supershifted by with the ARNT antibody (Figure 2C, lanes 6, 9, and 12). We conclude from these results that HIF-α stabilization, subcellular localization, and DNA binding activity are dependent upon the presence of functional pVHL regardless of O_2 concentration.

Loss of *Vhl* is sufficient to activate HIF-mediated transcription under normoxia

To assess the transcriptional activity of HIF in *Vhl*$^{-/-}$ ES cells, reporter assays using hypoxia response element (HRE)-driven luciferase constructs were performed (Figure 3A). Normoxic *Vhl*$^{+/+}$ and *Vhl*$^{+/-}$ ES cells demonstrated low levels of HIF transcriptional activity induced more than 10-fold by hypoxia. In contrast, although the levels of HIF activity varied between *Vhl*$^{-/-}$ clones within these assays, the trend consistently showed high

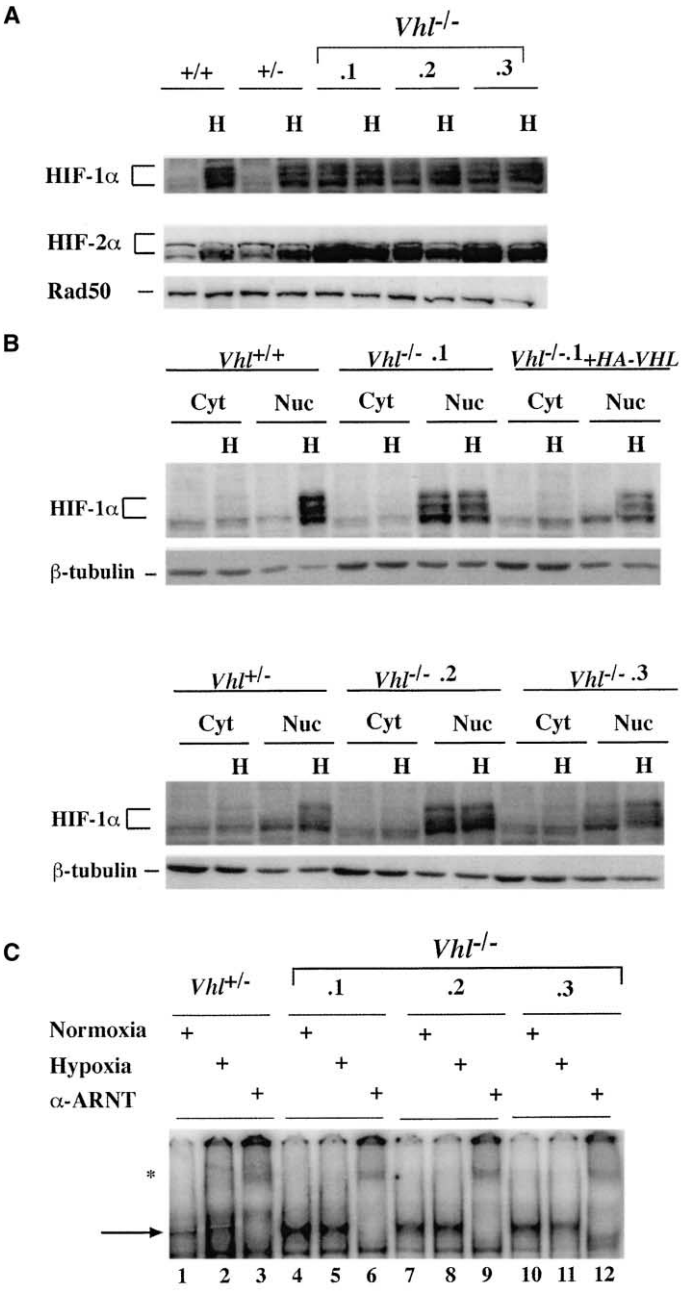

Figure 2. HIF stabilization and DNA binding activity in the absence of *Vhl*

A: Nuclear extracts were prepared from ES cells cultured under normoxia (21% O_2) or hypoxia (1.5% O_2) for 4 hr. Low levels of HIF-1α and HIF-2α proteins were present under normoxia and become markedly induced by hypoxia in $Vhl^{+/+}$ and $Vhl^{+/-}$ ES cells. In the absence of *Vhl,* HIF-α proteins became stabilized under normoxia at higher levels than $Vhl^{+/+}$ and $Vhl^{+/-}$ ES cells and were not substantially induced by hypoxia. Nuclear protein Rad50 was utilized as a loading control.

B: Immunoblot for HIF-1α in cytoplasmic and nuclear fraction revealed that stabilized HIF-1α accumulated exclusively in the nucleus of $Vhl^{-/-}$ ES cells. HIF-1α regulation was restored by stable transfection of HA-VHL into clone $Vhl^{-/-.1}$. Loading control β-tubulin, although more abundant in cytoplasmic fractions, demonstrated equivalent protein amounts were loaded per cell sample.

C: EMSA of 5.0 μg nuclear extracts prepared from cells grown under normoxic or hypoxic conditions for 4 hr where indicated. HIF DNA binding activity was maintained in $Vhl^{-/-}$ cells under normoxia. The arrow represents the HIF/ARNT complex, which was shown to be specific by supershifting with an α-ARNT antibody, marked by an asterisk.

levels of HIF activity under normoxic conditions, which were only slightly elevated by hypoxia. Use of a mutant HRE construct, which contains three base pair substitutions to disrupt HIF binding, ablated the hypoxic induction of transcriptional activity in all cell lines demonstrating its HIF dependence. Furthermore, *Hif-1*$\alpha^{-/-}$ ES cells exhibited reduced levels of luciferase activity in both normoxic and hypoxic conditions, comparable to levels detected using the mutant HRE construct. Importantly, cotransfection of a plasmid encoding HA-VHL with HRE-reporter constructs repressed normoxic HIF activity and restored hypoxic induction of HRE-dependent transcription in $Vhl^{-/-}$ cells (Figure 3B).

To further investigate the function of stabilized HIF in $Vhl^{-/-}$ cells, the activation of endogenous HIF target genes was examined. mRNA expression analysis of several known hypoxia-responsive genes (*Glut-1*, *Vegf*, *Pgk*, *Alda*, and *Bnip3)* revealed low levels of expression in normoxic $Vhl^{+/+}$ and $Vhl^{+/-}$ ES cells, which were markedly induced by hypoxia (Figure 4A). In direct contrast, the expression of HIF target genes in multiple normoxic $Vhl^{-/-}$ ES clones was comparable to, if not greater than, their expression in hypoxic $Vhl^{+/+}$ and $Vhl^{+/-}$ ES cells. Consistent with reporter gene data, HIF target gene expression remained high and was not greatly affected by hypoxia in two $Vhl^{-/-}$ ES clones. Clone $Vhl^{-/-.3}$ exhibited high levels of HIF target gene expression under normoxia that was moderately induced by hypoxia, albeit to a lesser degree than wild-type controls. This could be simply a result of clonal variation, as extensive genotyping indicated the absence of contaminating $Vhl^{+/-}$ cells in this clone. In all other assays that analyzed HIF target gene activation, $Vhl^{-/-.3}$ behaved similarly to the other clones. The expression of all target genes was primarily regulated by HIF, as shown by their greatly reduced expression in *Hif-1*$\alpha^{-/-}$ ES cells. However, *Glut-1* and *Vegf* transcripts can be stabilized by hypoxia independently of HIF (Ikeda et al., 1995; Levy et al., 1996a, 1996b), which may account for the residual hypoxic induction of these genes in *Hif-1*$\alpha^{-/-}$ ES cells.

To further assess the activation of HIF targets, VEGF secretion was measured by ELISA (Figure 4B). Although the absolute amounts of VEGF secretion varied between all clones, the pattern of *Vegf* regulation observed by Northern blot was recapitulated. VEGF secretion by $Vhl^{+/+}$ and $Vhl^{+/-}$ cells was substantially induced by hypoxia, while secretion by $Vhl^{-/-}$ cells under the same conditions remained similar to their normoxic levels. The induction of VEGF secretion by hypoxia could be restored by reintroduction of HA-VHL into clone $Vhl^{-/-.1}$.

When O_2 is limiting, cells switch from oxidative phosphorylation to glycolysis as the primary generator of ATP (Pasteur effect). Since the constitutive stabilization of HIF in $Vhl^{-/-}$ cells mimicked a hypoxic state, the glycolytic rate of and lactic acid production by these cells was measured. Consistent with their upregulation of glycolytic genes (*Glut-1, Pgk,* and *Alda*), $Vhl^{-/-}$ cells consumed more glucose than $Vhl^{+/+}$ and $Vhl^{+/-}$ cells over the course of a 1 hr normoxic incubation (Figure 4C). The higher glycolytic rate of $Vhl^{-/-}$ ES cells resulted in a substantially increased rate of lactate production over the course of 24 hr, when compared to $Vhl^{+/+}$ and $Vhl^{+/-}$ cells (Figure 4D). The increased glycolytic rate in and lactate production by $Vhl^{-/-.1}$ were suppressed by reintroduction of HA-VHL, demonstrating that these effects on glycolysis are pVHL dependent. Therefore, by the criteria of stabilization, nuclear localization, DNA binding activity, target gene activation, and cellular metabolism, loss of *Vhl*

A

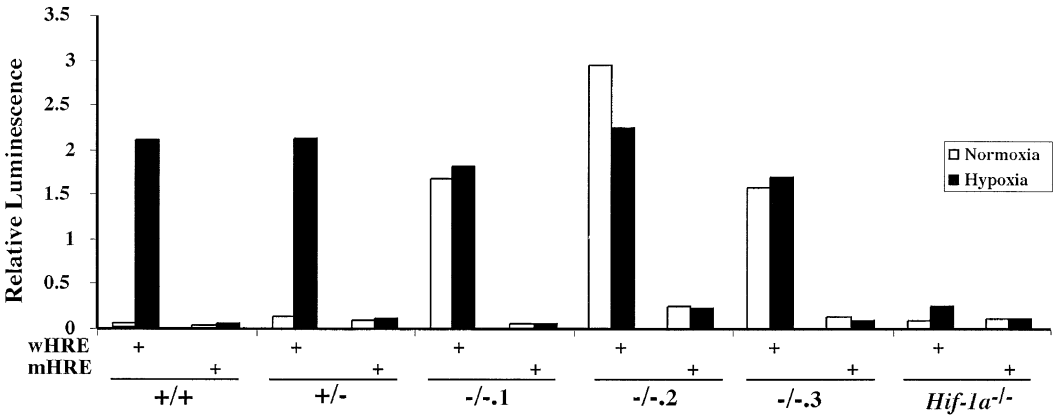

B

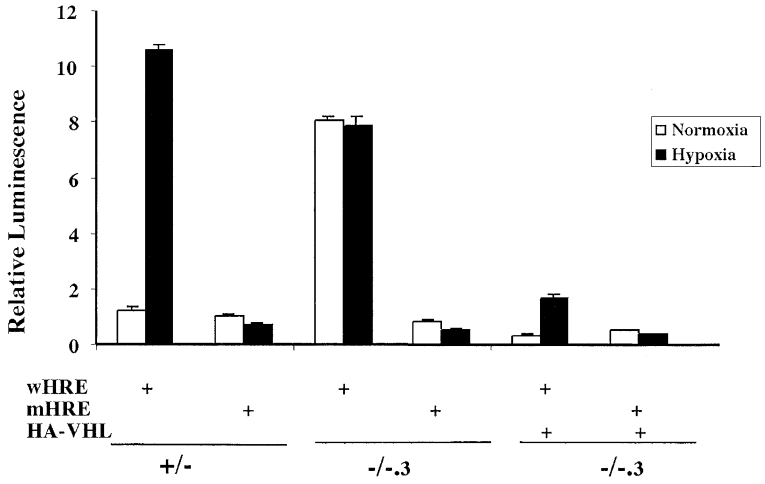

Figure 3. HIF transcriptional activity is dysregulated in *Vhl*$^{-/-}$ ES cells

A: ES cells were transiently transfected with wild-type (wHRE) or mutant (mHRE) reporter constructs, and transcriptional activity was measured in normoxic (21% O_2) or hypoxic (1.5% O_2) cells at 16 hr. Luciferase activity detected in normoxic *Vhl*$^{-/-}$ clones was not further induced by hypoxia. Data represent one of three independent assays in which similar results were produced.

B: ES cells were cotransfected with wHRE or mHRE plus or minus a plasmid encoding HA-VHL. The presence of HA-VHL decreased the normoxic levels of HIF activity and restored hypoxic induction. Assays were performed in triplicate and bars represent standard error.

alone is sufficient to constitutively activate HIF to hypoxic levels, independent of O_2 signaling.

Loss of *Vhl* does not promote tumor growth

To investigate whether loss of *Vhl* can enhance the tumorigenic potential of ES cells, subcutaneous tumors were generated by injecting *Vhl*$^{+/-}$ and *Vhl*$^{-/-}$ ES cells into the dorsal region of NIH-III immunodeficient mice. Clones *Vhl*$^{-/-.1}$ and *Vhl*$^{-/-.2}$ were used because of their high levels of VEGF secretion relative to *Vhl*$^{+/-}$ cells (Figure 4B). Surprisingly, *Vhl*$^{-/-}$ tumors were considerably smaller than *Vhl*$^{+/-}$ tumors after 21 or 28 days. Table 1 shows the results of four separate experiments in which *Vhl*$^{-/-}$ tumors were on average 42%–68% smaller than *Vhl*$^{+/-}$ tumors. *Vhl*$^{-/-.1}$ tumors grew more slowly than *Vhl*$^{+/-}$ controls as measured by tumor volume, contrary to the findings of pVHL-deficient RCC-derived tumors (Figure 5B) (Iliopoulos et al., 1995). Figure 5C shows pooled data from three separate teratocarcinoma experiments at 21 days, in which the masses of tumors formed by

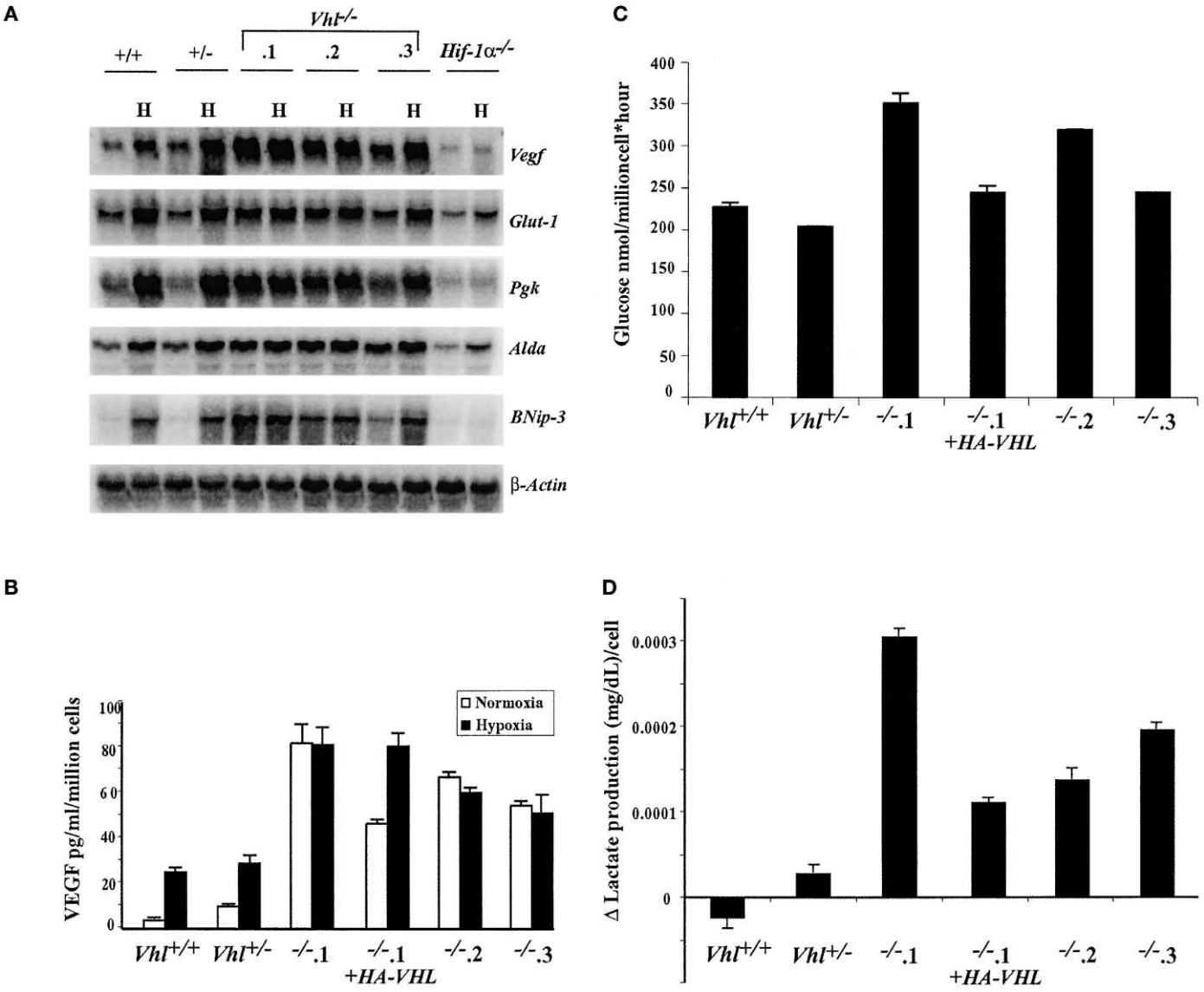

Figure 4. Induction of HIF target genes in normoxic *Vhl*$^{-/-}$ ES cells

A: Total RNA isolated from *Vhl*$^{+/+}$, *Vhl*$^{+/-}$, *Vhl*$^{-/-}$ clones and *Hif-1α*$^{-/-}$ ES cells was probed for *Vegf*, *Glut-1*, *Pgk*, *Alda*, *Bnip-3*, and β-*actin*, which served as a loading control. Expression of HIF target genes was abundant under normoxia and failed to be further induced by hypoxia in *Vhl*$^{-/-}$ ES clones.

B: In vitro secretion of VEGF was measured by ELISA. VEGF secretion was greatly induced by hypoxia in *Vhl*$^{+/+}$ and *Vhl*$^{+/-}$ ES cells but not in *Vhl*$^{-/-}$ clones. The high level of VEGF secretion by *Vhl*$^{-/-.1}$ was suppressed by reintroduction of HA-VHL.

C: A representative measurement of the glycolytic rate assessed as the rate of conversion of ^{3}H-Glucose to $^{3}H_2O$ (Liang et al., 1997). *Vhl*$^{-/-}$ ES cells consumed glucose at a higher rate than controls, and this phenotype was suppressed by reintroduction of HA-VHL.

D: Change in lactate secretion measured over the course of 24 hr is depicted. *Vhl*$^{-/-}$ ES cells secreted greater amounts of lactate than controls; this phenotype was also suppressed by reintroduction of HA-VHL. All assays were performed in triplicate and bars represent standard error.

clones *Vhl*$^{-/-.1}$ and *Vhl*$^{-/-.2}$ were combined for an N value of 20. The difference between the masses of *Vhl*$^{+/-}$ and *Vhl*$^{-/-}$ tumors was statistically significant ($p = 0.003$ by Student's t test). Most importantly, the growth of genetically rescued *Vhl*$^{-/-.1}$ + HA-VHL tumors was similar to *Vhl*$^{+/-}$ controls, demonstrating that this deficiency is functionally dependent upon *Vhl* (Figure 5C).

Microvessel density is increased in *Vhl*$^{-/-}$ tumors

Gross morphological analysis revealed a higher incidence of hemorrhagic regions within *Vhl*$^{-/-}$ tumors (Figures 6A and 6B). In addition, primitive tissues derived from all three germ layers were present in *Vhl*$^{-/-}$ tumors; however, more differentiated tissue types such as skeletal muscle, cartilage, neuronal axons, adipocytes, and secretory glands were absent or extremely rare, compared to *Vhl*$^{+/-}$ tumors (data not shown). The presence of a subset of these tissues was restored in *Vhl*$^{-/-.1}$ + HA-VHL tumors (data not shown). The ability of *Vhl*$^{-/-}$ ES cells to deposit fibronectin in the extracellular matrix was assessed by immunohistochemistry. *Vhl*$^{+/-}$ tumors exhibited abundant fibronectin staining in the basement membrane of blood vessel endothelial cells (Figure 6C). Fibronectin staining within *Vhl*$^{-/-}$ tumors was greatly reduced in this cell type (Figure 6D), consistent with

Table 1. *Vhl*$^{-/-}$ tumors are smaller than controls

	Genotype	T/S[a]	Days	Mean Mass (g)
Exp. 1	*Vhl*$^{+/-}$	6/6	21	3.052 ± 0.670
	Vhl$^{-/-.1}$	5/6	21	1.036 ± 0.257
Exp. 2	*Vhl*$^{+/-}$	10/10	21	1.223 ± 0.238
	Vhl$^{-/-.2}$	10/10	21	0.709 ± 0.092
Exp. 3	*Vhl*$^{+/-}$	5/5	21	1.62 ± 0.371
	Vhl$^{-/-.1}$	4/4	21	0.53 ± 0.125
	Vhl$^{-/-.1}$ + *HA-VHL*	5/5	21	1.76 ± 0.296
Exp. 4	*Vhl*$^{+/-}$	5/5	28	4.96 ± 1.19
	Vhl$^{-/-.1}$	3/4	28	0.466 ± 0.318

[a]T/S, number of tumors formed/number of sites injected.

previously reported data for RCCs and *Vhl*$^{-/-}$ embryos (Ohh et al., 1998; Hoffman et al., 2001). Histological staining for an endothelial cell-specific antigen (CD34) to demarcate tumor vasculature indicated an increase in microvessel density of *Vhl*$^{-/-}$ tumors (47.5 microvessels/mm^2 ± 5.0) when compared to *Vhl*$^{+/-}$ tumors (23.1 microvessels/mm^2 ± 3.1) (Figures 6E and 6F). This statistically significant difference correlated with increased VEGF secretion by *Vhl*$^{-/-}$ cells in vitro and is consistent with data reported for RCC-derived tumors (Kondo et al., 2002) ($p = 0.0256$ by Student's t test) (Figure 6G). When compared to controls, the phenotype of *Vhl*$^{-/-}$ teratocarcinomas paralleled that of *VHL*$^{-/-}$ RCCs in terms of fibronectin deposition and microvessel density. However, pVHL-deficient teratocarcinomas are smaller than controls, emphasizing a discontinuity between angiogenesis and tumor proliferation.

Vhl$^{-/-}$ tumors are deficient in proliferation but do not exhibit an increase in apoptosis

A possible mechanism for the reduction in tumor volume and mass could be a decrease in cell growth or an increase in cell death. Although undifferentiated *Vhl*$^{-/-}$ cells do not exhibit these defects in vitro (data not shown), growth in an in vivo tumor microenvironment might reveal such a phenotype. Teratocarcinoma sections were therefore assessed for expression of cell cycle markers. Immunostaining for the proliferation marker Ki-67 (present in the nuclei of all cells not in G0) revealed highly proliferating regions in *Vhl*$^{+/-}$ tumors, most notably in ectoderm-derived tissue (Figure 7A). Examination of similar tissue types within *Vhl*$^{-/-}$ tumors also revealed Ki-67 positive staining, but at lower levels (Figure 7B). Morphometric analysis of these regions revealed that 41.5% of cells within *Vhl*$^{-/-}$ tumors were Ki-67$^+$ as compared to 68.1% in *Vhl*$^{+/-}$ tumors and 60.2% in the genetically rescued tumors *Vhl*$^{-/-.1}$+ HA-VHL (Figure 7C), a statistically significant difference ($p = 0.0028$ by Student's t test). This reduction in proliferation rate, although modest, may account for the slower growth rate of *Vhl*$^{-/-}$ tumors over the course of 21 days.

A concomitant increase in the rate of apoptosis could also cause the reduced mass of *Vhl*$^{-/-}$ teratocarcinomas. To assess this possibility, sections were stained for the apoptotic marker cleaved caspase-3. Although *Vhl*$^{-/-}$ tumors were significantly smaller than *Vhl*$^{+/-}$ tumors, there was no corresponding increase in apoptosis outside of necrotic regions (Figures 7D and 7E). Morphometric analysis did not reveal any differences between the number of cleaved caspase-3$^+$ cells in *Vhl*$^{-/-}$ and *Vhl*$^{+/-}$ sections (2.56% and 2.97%, respectively) (Figure 7F). In addition, apoptosis assessed by TUNEL staining (Figures 7G and 7H), did not reveal any quantitative differences between *Vhl*$^{-/-}$ and *Vhl*$^{+/-}$ tumors (4.67% and 4.47%, respectively) when normalized to DAPI-stained nuclei (Figures 7I–7K). Although the percentage of TUNEL$^+$ cells was greater than that of cleaved caspase-3$^+$ cells, neither apoptosis detection method revealed significant differences between the tumor types. We conclude that although loss of *Vhl* is sufficient to dysregulate HIF, this alone does not promote teratocarcinoma growth in a subcutaneous tumor model. To the contrary, loss of *Vhl* seems to impair the growth of primary cells in vivo.

Discussion

Loss of the tumor suppressor *VHL* is correlated with the development of highly vascularized tumors within the kidney, central nervous system, and retina (Maher and Kaelin, 1997). Insight into *VHL*'s role as a tumor suppressor can be found in its ability to bind and target HIF-α subunits for ubiquitin-mediated degradation (Maxwell et al., 1999; Cockman et al., 2000; Tanimoto et al., 2000). We have shown that whereas loss of *Vhl* is sufficient to completely dysregulate HIF, it does not enhance the growth of subcutaneous tumors derived from primary cells. In contrast, *VHL*$^{-/-}$ RCC cells produce in nude mice rapidly growing xenografts, the growth of which is suppressed by reintroduction of functional pVHL. The combined effects of pVHL deficiency and additional mutations within the RCC cells may explain this apparent discrepancy.

The activation of HIF is thought to be an O_2-regulated, multistep pathway requiring α subunit stabilization, nuclear translocation, and recruitment of coactivators (Jiang et al., 1997; Pugh et al., 1997; Kallio et al., 1999; Tanimoto et al., 2000; Lando et al., 2002). Recent evidence also suggests that full activation of HIF is not only dependent upon inhibition of HIF-α prolyl hydroxylation but also asparagyl hydroxylation within the C-terminal activation domain (CAD) (Lando et al., 2002; Sang et al., 2002). In our studies, normoxic *Vhl*$^{-/-}$ ES cells displayed constitutive HIF-α stability and HIF activity, neither of which were substantially induced by hypoxia. The nuclear accumulation of stabilized HIF-1α seen in *Vhl*$^{-/-}$ cells is consistent with a recent report suggesting that HIF-1α nuclear export is pVHL dependent (Groulx and Lee 2002). Constitutively stabilized HIF-1α in *Vhl*$^{-/-}$ cells maintained DNA binding activity and maximally stimulated the expression of downstream target genes. Proper HIF regulation was restored by genetic rescue with HA-VHL. Hence, loss of *Vhl* leads to the full activation of HIF in ES cells, even in the absence of additional hypoxic signaling.

Reintroduction of wild-type *VHL* suppresses the growth of pVHL-deficient RCC tumors in nude mice (Gnarra et al., 1996; Iliopoulos et al., 1996). In contrast, expression of pVHL containing β domain mutations that disrupt pVHL/HIF-α interaction does not suppress tumor formation, highlighting the importance of HIF regulation for the tumor suppressor function of *VHL* (Bonicalzi et al., 2001). pVHL-rescued RCC cells expressing constitutively stabilized HIF-1α produce smaller tumors than those derived from the parental RCC cell line, indicating that loss of *VHL* contributes to tumor growth through HIF-1α-independent mechanisms (Maranchie et al., 2002). Interestingly, HIF-2α is more frequently upregulated than HIF-1α in renal clear cell carcinomas (Turner et al., 2002) and has been implicated as a critical target for *VHL*-mediated tumor suppression in renal clear cell

A

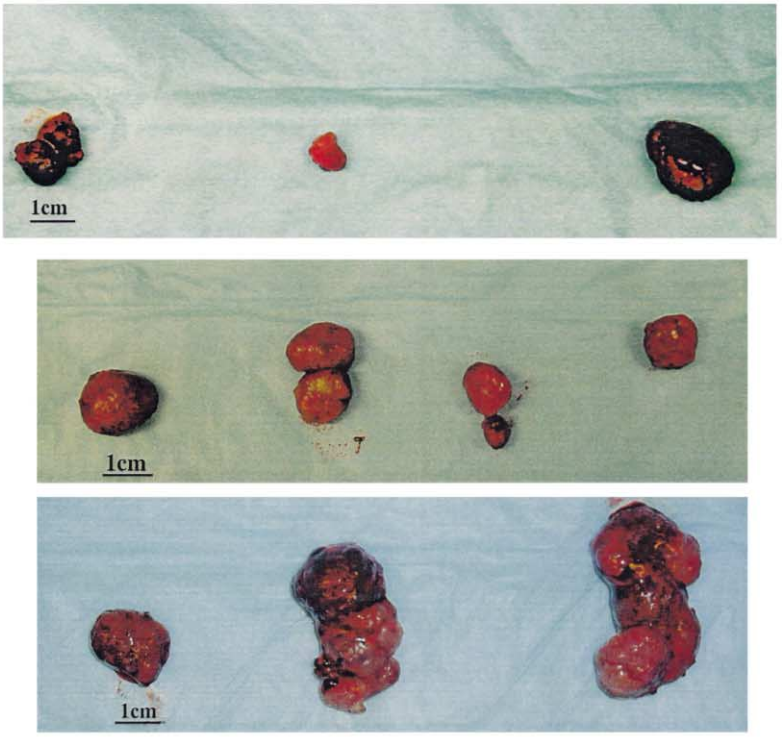

Vhl$^{-/-}$.1

Vhl$^{-/-}$.2

Vhl$^{+/-}$

B

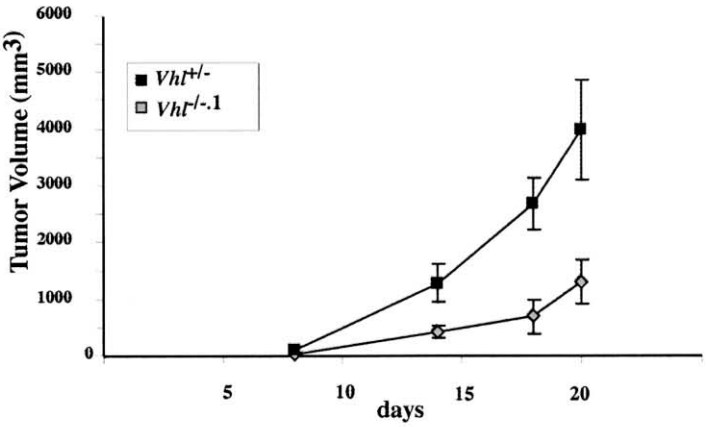

C

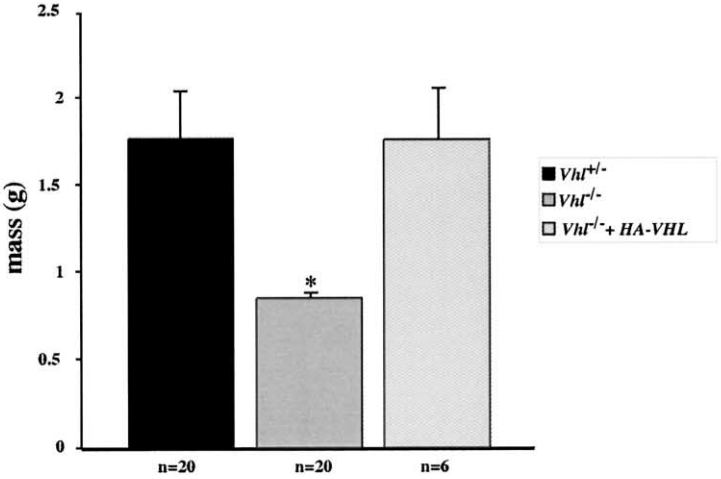

carcinomas. Our results suggest that constitutive activation of HIF transcriptional activity in *Vhl*$^{-/-}$ ES cell-derived teratocarcinomas promotes tumor angiogenesis, but is itself insufficient to increase tumor growth. This may reflect the fact that our targeted *Vhl*$^{-/-}$ ES cells differ fundamentally from pVHL-deficient RCC cell lines in at least one important way; specifically, they have not undergone selection in vivo for the ability to overcome proliferation checkpoints and apoptotic controls known to suppress tumorigenesis. The chromosomal abnormalities observed in RCC cell lines (Gunawan et al., 2001) are consistent with the idea that genetic instability underlies the multiple genetic hits that facilitate tumor formation (Hanahan and Weinberg 2000). In contrast, the use of *Vhl*$^{-/-}$ ES cells permits assessment of pVHL function in an intact genetic background. Taken together, these results suggest that the tumorigenic phenotype of RCC cell lines requires not only pVHL's HIF-dependent and HIF-independent functions, but also other oncogenic mutations.

The precise role of HIF in tumor development is controversial due to the conflicting results of several tumor models. While one group found that genetic disruption of the *Hif-1*α locus results in the accelerated growth of poorly vascularized *Hif-1*$\alpha^{-/-}$ teratocarcinomas (Carmeliet et al., 1998), others have shown that the absence of HIF activity in teratocarcinomas and fibrosarcomas impairs tumor growth, but not tumor angiogenesis (Ryan et al., 1998, 2000; Hopfl et al., 2002). Additional support for HIF as a positive regulator of tumor growth has been obtained from tumor models using nonprimary cells. In three different tumor cell lines, loss or disruption of HIF activity also inhibits expression of HIF target genes, tumor vasculature, and growth (Maxwell et al., 1997; Kung et al., 2000; Hopfl et al., 2002). Disrupted binding of HIF to coactivators p300 and CBP can also attenuate tumor growth (Kung et al., 2000). Therefore, the full oncogenic consequences of HIF dysregulation are still unresolved and will probably depend considerably on genetic background.

The meager growth of *Vhl*$^{-/-}$ teratocarcinomas, a rather unexpected phenotype considering *VHL*'s role as a tumor suppressor, did not result from increased apoptosis in *Vhl*$^{-/-}$ ES cell-derived tumors. This point was of particular interest, as the proapoptotic gene *Bnip-3* has recently been described as a novel HIF transcriptional target (Bruick 2000; Sowter et al., 2001). In fact, *Bnip-3* expression has been shown to be stimulated in hypoxic regions of human tumors (Sowter et al., 2001). Although the mRNA transcript of *Bnip-3* was highly expressed in both normoxic and hypoxic *Vhl*$^{-/-}$ cells (Figure 4A), this did not equate with an increase in cell death or a growth disadvantage in vitro. In fact, doubling time and S phase composition as measured by propidium iodide incorporation of *Vhl*$^{-/-}$ cells did not differ significantly from *Vhl*$^{+/+}$ or *Vhl*$^{+/-}$ cells (data not shown). Furthermore, cleaved caspase-3 and TUNEL staining did not reveal an increase in apoptosis in *Vhl*$^{-/-}$ teratocarcinomas (Figures 7D–7I). These results suggest that the expression of *Bnip-3* in undifferentiated and differentiated ES cells does not induce apoptosis.

Vhl's effects on early development and tumor growth are contrary to those found for other tumor suppressors such as PTEN. Loss of PTEN also results in embryonic lethality, but still enhances the growth of tumors derived from primary ES cells and embryonic fibroblasts (Di Cristofano et al., 1998; Stiles et al., 2002). The aberrant differentiation of *Pten*$^{-/-}$ cells, although detrimental to early development, is actually beneficial for tumor proliferation. In contrast, loss of *VHL* may only be able to induce tumor growth in a background of genetic changes. Cytogenetic abnormalities have been observed in RCC cells, and a minority of RCCs and RCC-derived cell lines have been shown to harbor p53 mutations (Reiter et al., 1993). Amplifications of the oncogenes c-*myc* and K-ras may also play a role in the generation of renal clear cell carcinomas (Kozma et al., 1997).

It is important to note that our teratocarcinoma model does not recreate the selective pressures that generate pVHL-deficient human cancers. In many ways, the development of heterogeneous tissues within teratocarcinomas reflects the differentiation of ES cells in early embryogenesis. Loss of *Vhl* in early development results in growth retarded embryos, which die between days E10.5–E12.5 (Gnarra et al., 1997). *Vhl*$^{-/-}$ teratocarcinomas, although less proliferative, appear to contain more primitive tissue types when compared to controls (data not shown). The decreased growth and differentiation of *Vhl*$^{-/-}$ teratocarcinomas suggests that pVHL may be required for the proliferation and/or initial differentiation of primary cells. For example, recent studies from our lab indicate that *Vhl*$^{-/-}$ ES cells generate reduced numbers of hematopoietic progenitors in in vitro assays (F.A.M. and M.C.S., unpublished data). In conclusion, our data suggest that although inactivation of *VHL*'s tumor suppressor functions can contribute to the malignancy of renal cancer, disruption of these same pathways in pluripotent cells appears to be detrimental to their growth and/or differentiation.

Experimental procedures

Generation and genotyping of Vhl$^{+/-}$ ES cells

5.0×10^4 *Vhl*$^{+/-}$ ES cells were plated on 10 cm gelatin-coated tissue culture dishes in media containing 4.0 mg/ml of G418 to promote loss of the second wild-type *Vhl* allele. Resistant clones were isolated and expanded after 6–7 days of selection. Genomic DNA extracted from cultured ES cells were digested with HindIII for Southern blot analysis using a probe generated from an AccI/XbaI fragment from the *Vhl* 3′ UTR. PCR was also used to genotype ES clones. Oligonucleotide primers included those specific for wild-type *Vhl* exon 3, 5′-ACT GAA AAC GTC TTC CTC CCT CGG G (reverse) and wild-type exon 1, 5′-GCG GAA GGA CAT ACA GCG ACT GAG CC-3′ (forward), and internal neo sequence 5′-TGA CTA GGG GAG GAG TAG AAG GTG GCG-3′ (reverse).

Figure 5. Decrease in growth of *Vhl*$^{-/-}$ tumors

A: Teratocarcinomas were created by injecting *Vhl*$^{+/-}$, *Vhl*$^{-/-.1}$, and *Vhl*$^{-/-.2}$ ES cells subcutaneously into nude mice. *Vhl*$^{-/-}$ tumors ranged in size but were considerably smaller than *Vhl*$^{+/-}$-derived tumors.

B: Rate of tumor growth was measured by tumor volume for 21 days.

C: Graph represents the combined results of three separate experiments in which the masses of *Vhl*$^{+/+}$, *Vhl*$^{-/-}$, and *Vhl*$^{-/-.1}$+ HA-VHL tumors after 21 days of growth were measured. N values are as indicated and bars represent standard error. *Vhl*$^{-/-}$ tumors were significantly smaller than *Vhl*$^{+/-}$-derived tumors. Genetically rescued *Vhl*$^{-/-.1}$ + HA-VHL tumors grew similarly to *Vhl*$^{+/-}$ tumors. Student's t test revealed a statistically significant difference between tumor masses, $p = 0.003$.

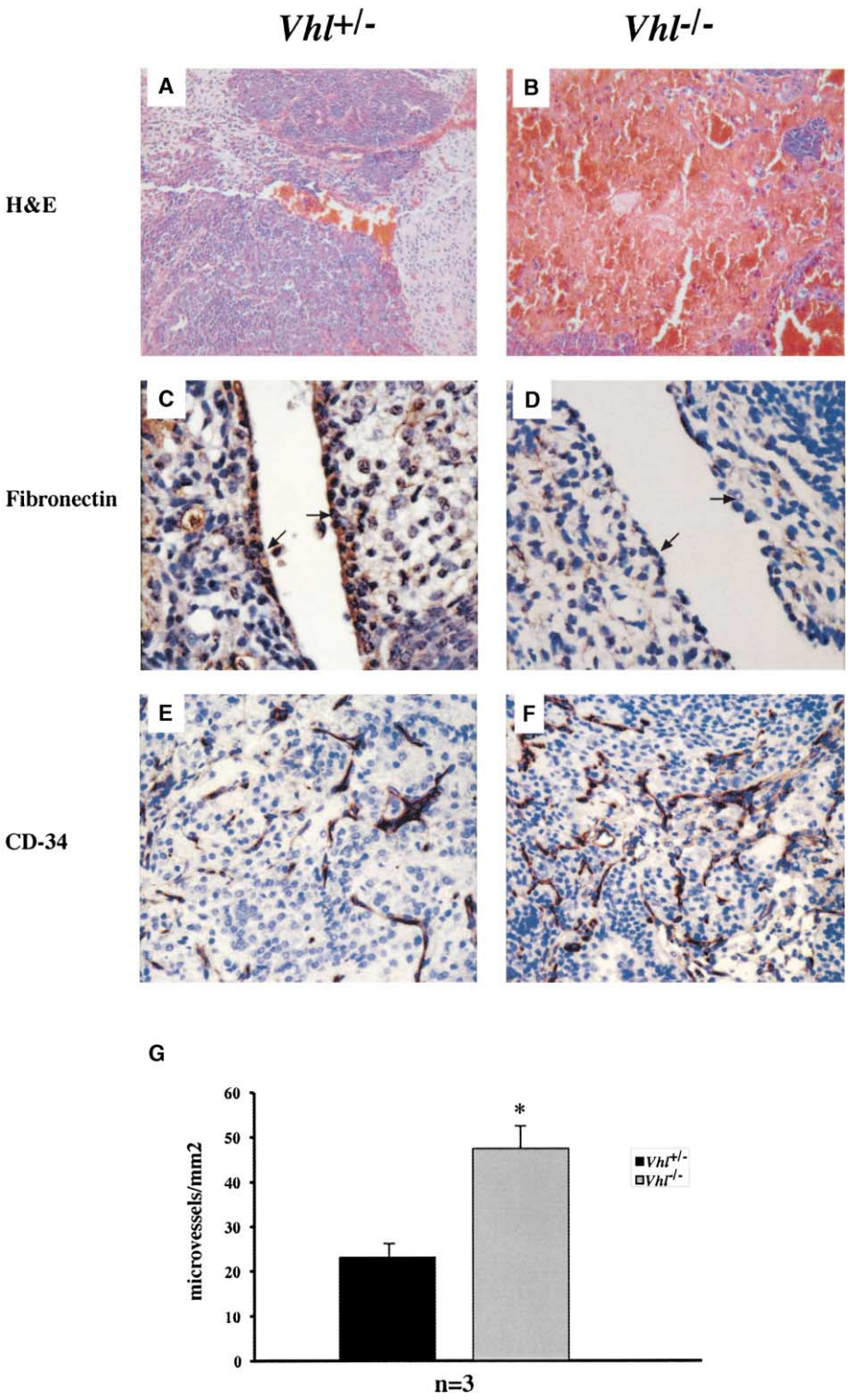

Figure 6. Increased hemorrhagic regions and vasculature of $Vhl^{-/-}$ tumors

A and **B:** Hematoxylin and eosin staining of $Vhl^{+/-}$ and $Vhl^{-/-}$ tumors.

C and **D:** Basement membrane expression of fibronectin in $Vhl^{+/-}$ endothelial cells (arrows) and reduced fibronectin deposition in endothelial cells of $Vhl^{-/-}$ tumors (arrows).

E: CD-34 staining of $Vhl^{+/-}$ microvessels.

F: Microvessel density in $Vhl^{-/-}$ tumors appeared to be increased as demonstrated by α-CD-34 staining.

G: Quantitation of tumor microvessel density. The microvessel density of $Vhl^{-/-}$ tumors was greater than controls, n = 3. Student's t test revealed statistically significant differences between tumor types, $p < 0.03$. Bars represent standard error. Final magnifications are 100× (**A** and **B**), 400× (**C** and **D**), and 200× (**E** and **F**).

Generation of rescued ES cell lines

Wild-type human cDNA encoding pVHL with an N-terminal hemagglutin epitope tag (HA-VHL) was obtained as a generous gift from Dr. W. Kaelin. 2×10^7 $Vhl^{-/-.1}$ ES cells were electroporated with 20 μg of PvuII linearized expression construct Station II containing HA-VHL with an SV-40 polyadenylation sequence at the C terminus. Resistant clones were screened by Southern blot using a 900 bp probe generated from a HindIII-EcoRI fragment from HA-tagged VHL cDNA. Clones with evidence of an integration event were further analyzed by Western blot.

Western blot analysis

For all Western blot and EMSA analyses, 6–7 × 10^6 cells were plated on 10 cm gelatin coated tissue culture dishes such that the density of the cells at the time of lysis was ~60%–70% confluent. Hypoxia, defined as 1.5% O_2,

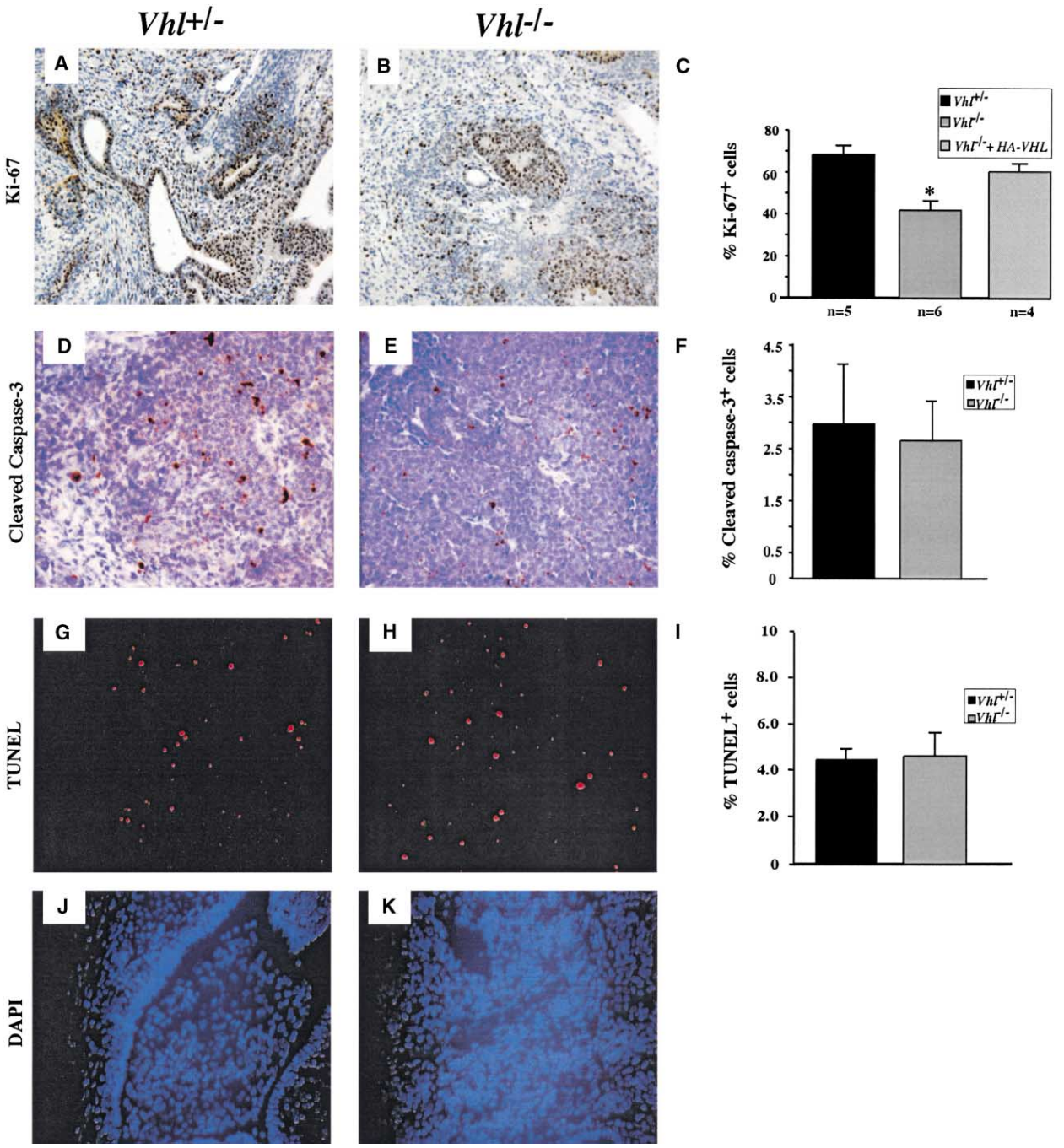

Figure 7. *Vhl*$^{-/-}$ tumors exhibited a decrease in proliferation but no increase in apoptosis

A: Proliferation marker Ki-67 indicated highly proliferating regions of *Vhl*$^{+/-}$ tumors.
B: Expression of Ki-67 in *Vhl*$^{-/-}$ tumors was reduced compared to morphologically similar *Vhl*$^{+/-}$ regions.
C: Quantitation of Ki-67^{+} cells in *Vhl*$^{+/-}$, *Vhl*$^{-/-}$, and *Vhl*$^{-/-}$ + HA-VHL tumors. *Vhl*$^{-/-}$ tumors were less proliferative than controls. Student's t test revealed statistically significant differences between tumors types, $p < 0.003$.
D and **E:** Expression of apoptotic marker cleaved caspase-3 in non-necrotic regions of *Vhl*$^{+/-}$ tumors. Cleaved caspase-3 staining was not increased in *Vhl*$^{-/-}$ tumors.
F: Quantitation of cleaved caspase-3^{+} cells in *Vhl*$^{+/-}$ and *Vhl*$^{-/-}$ tumors. No significant differences were observed between genotypes.
G and **H:** TUNEL staining demarcated apoptotic cells in non-necrotic regions of *Vhl*$^{+/-}$ and *Vhl*$^{-/-}$ tumors.
I: Quantitation of TUNEL^{+} cells in *Vhl*$^{+/-}$ and *Vhl*$^{-/-}$ tumors. No significant differences were apparent between genotypes. N values are as indicated and bars represent standard error. Magnifications 200× (**A–H**).
J and **K**: Corresponding DAPI staining of TUNEL^{+} regions in **G** and **H**. Magnification 200×.

was generated using an In Vivo$_2$ hypoxic workstation (Ruskinn Technologies, Leeds, United Kingdom) for Western and EMSA analyses, or an IG750 variable O_2 tissue culture incubator (Jouan Inc.) for reporter and Northern analyses.

Whole-cell protein lysates were prepared using WCE buffer: 150 mM NaCl, 50 mM Tris (pH 7.4), 5 mM EDTA, 0.1% SDS, and Complete Protease Inhibitor (Roche Molecular Biochemicals). Nuclear and cytoplasmic fractions of protein extracts were prepared using a modified Dignam protocol (Maltepe et al., 2000) with Buffer A further modified to contain 0.1% NP-40 and Buffer C containing 300 mM NaCl. For hypoxic extracts, cells were manipulated inside a hypoxic chamber using phosphate-buffered saline and Buffer A that had been equilibrated to the hypoxic environment. Extracts were electrophoresed, transferred, and immunoblotted according to standard protocols using 5% nonfat dry milk (Carnation) in Tris-buffered saline/Tween 20 as a blocking agent. Blots were stained with Ponceau S to ensure equal loading. Antibodies used include: α-mouse pVHL (Santa Cruz), α- human pVHL (Pharmingen), α- mouse HIF-1α and HIF-2α (Novus), α-mouse Rad-50 (Transduction Laboratories), and α-mouse β-tubulin (InnoGenex). Horseradish peroxidase-conjugated α-rabbit and α-mouse secondary antibodies were purchased from Cell Signaling Technologies and used at dilutions of 1:2000. ECL reagents were purchased from Amersham Biosciences. Blots were stripped in 61.5 mM Tris (pH 6.8), 2% SDS, and 100 mM β-mercaptoethanol at 55°C for 1 hr before being blocked and re-probed.

Electrophoretic mobility shift assay (EMSA)

EMSA analyses have been previously described (Maltepe et al., 2000). In brief, 5 μg of nuclear extracts were incubated in binding buffer consisting of 10 mM Tris-HCl (pH 7.5), 50 mM NaCl, 50 mM KCl, 1 mM $MgCl_2$, 5 mM dithiothreitol, 1 mM EDTA, and 5% glycerol to which 0.05 mg/ml bovine serum albumin, 0.025 μg/ml of CREB oligo, 10^6 dpm of labeled probe, and, where indicated, 0.5 μl of polyclonal α-ARNT antiserum (Novus) were added. The 24 bp oligonucleotide probe was derived from the erythropoietin HRE, 5′-GCC CTA CGT GCT GTC CTC A-3′.

Reporter assays

The HRE-luciferase reporter constructs were previously described (Arsham et al., 2002). Transfection efficiency was assessed by cotransfection of a renilla luciferase gene under the control of a minimal tyrosine kinase promoter. Where indicated, cells were also cotransfected with plasmid encoding HA-tagged full-length human pVHL. For transient tansfections, 2×10^6 ES cells were plated on gelatin-treated 6-well plates and allowed to recover overnight. Cells were transfected the next morning using Lipofectamine Plus reagent (Gibco BRL) according to manufacturer's protocol. Cells were transfected for 4 hr and one half of each sample was exposed to hypoxia for 18 hr. Proteins were extracted from samples using reporter lysis buffer and dual luciferase assays were performed according to manufacturer's guidelines (Promega).

Northern analysis

For Northern blots, 2–3 $\times$ 10^6 cells/10 cm tissue culture dish were plated and allowed to recover overnight. Where indicated, cells were incubated in hypoxia for 18 hr. All cells were lysed in Trizol (Invitrogen) according to manufacturer's instructions in ambient air. Twenty micrograms of total RNA were electrophoresed in 1.5% denaturing (formaldehyde) agarose gels and transferred to Hybond N+ membranes (Amersham). Murine *Vegf*, *Pgk*, *Alda*, and *Glut-1* probes have been previously described (Maltepe et al., 1997). Murine *Bnip3* probe was generated by RT-PCR from cDNA synthesized from murine FL5.12 cell RNA. A 738 bp fragment was amplified between bp11 and 749 using primers 5′TGC CCC TGC TAC CTC TCG (forward) and 5′ CAT AGT GCA AAC ACC CAA GG (reverse). PCR products were sequenced and confirmed to be identical to GenBank sequence NM_009760 for murine *Bnip3*.

VEGF ELISA

VEGF quantitation was performed using the Quantikine M Murine Immunoassay kit, (R&D Systems) according to manufacturer's protocol. 7.5×10^5 cells were seeded on gelatin coated 12-well plates and incubated in hypoxia for 18 hr where indicated. Conditioned medium was incubated with a mouse-specific VEGF polyclonal antibody bound to a microtiter plate. After several washes, a second enzyme-linked polyclonal antibody specific for mouse VEGF was added. Sample values were obtained according to manufacturer's protocol. Recorded values were normalized for cell number.

Glycolytic rate assay

Glycolysis was assayed as the rate of conversion of ^{3}H-Glucose to ^3H_2O as previously described (Liang et al., 1997). 1×10^6 cells were washed once in PBS and media were replaced with 0.5 ml of Krebs buffer and incubated for 30 min at 37°C. Krebs buffer was then replaced with 0.5 ml of Krebs buffer containing 10 mM glucose and spiked with 10 μCi of 5-^{3}H-glucose. Following incubation for 1 hr at 37°C, triplicate 50 μl aliquots were transferred to uncapped PCR tubes containing 50 μl of 0.2N HCl, and these tubes were transferred to scintillation vials containing 0.5 ml of H_2O such that the water in the vial and the contents of the PCR tubes were not allowed to mix. The vials were sealed and diffusion was allowed to occur for 48 hr. The amounts of diffused and undiffused ^{3}H were determined by scintillation counting. Appropriate ^{3}H-glucose-only and ^3H_2O-only controls were included, enabling the calculation of ^3H_2O in each sample and thus the rate of glycolysis.

Lactate secretion assay

Lactate concentrations were indirectly determined by a colorimetric assay, which converts the lactic acid present in the media into H_2O_2, resulting in the oxidative condensation of a chromogen precursor (Sigma). Approximately 5×10^4 cells were plated on gelatin coated 24-well plates and allowed to recover overnight. Samples were collected and individual cell counts were obtained every 24 hr for 2 days thereafter.

Mouse teratocarcinoma assay

5×10^6 cells were suspended in 100 μl of phosphate-buffered saline (Gibco) and injected subcutaneously into the dorsal area of 4- to 6-week-old female NIH-III immunodeficient mice (Taconic). After 7 days, tumors were measured every 2–3 days with calipers in the two greatest dimensions to calculate tumor volume. After 21 or 28 days, tumors were excised, photographed, weighed, frozen for protein assays, and fixed in 4% paraformaldehyde.

Immunohistochemistry

Tumor samples were fixed in 4% paraformaldehyde and paraffin embedded by standard techniques. Six micrometer sections of each sample were incubated overnight with antibodies generated against fibronectin (BD Scientific), cleaved caspase-3 (Calbiochem), Ki-67 (Novacastra), and CD-34 (BD Scientific). A TUNEL assay *In Situ* Cell Death Detection Kit was utilized according to the manufacturer's protocol (Roche). α-mouse and α-rat secondary antibodies were biotinylated and staining achieved by a strepavidin-biotin system conjugated with horseradish peroxidase (Vector Lab). Fibronectin, CD-34, and cleaved caspase-3 photographs were taken with a Nikon N6006 35 mm camera. Ki-67 photographs were taken with a Spot RT slider digital camera (Diagnostic Instruments Inc.) with a magnification of 0.76×. Morphometric analysis was performed on three to five randomly chosen sections of each tumor using the analytical program Image Pro (Phase 3 Imaging). The number of positive cells was calculated as the total area of positive staining divided by the area of an individual positive cell. The percentage positive cells were calculated as the number of positive cells divided by the total number of cells.

Acknowledgments

We thank Min-min Lu, Q.C. Yu, Cynthia Clendenin, Clint Culpepper, Frank Winslow, Marian Harris, J Thompson, Aaron Gitler, and Nathalie Innocent for reagents and technical assistance. This research was supported by National Institute of Health Grants HL63310 (M.C.S.) and 1F31HD (F.A.M.) and the Abramson Family Cancer Research Institute. M.C.S. is an investigator at the Howard Hughes Institute.

Received: August 1, 2002
Revised: December 5, 2002

References

Arany, Z., Huang, L.E., Eckner, R., Bhattacharya, S., Jiang, C., Goldberg, M.A., Bunn, H.F., and Livingston, D.M. (1996). An essential role for p300/

CBP in the cellular response to hypoxia. Proc. Natl. Acad. Sci. USA *93*, 12969–12973.

Arsham, A.M., Plas, D.R., Thompson, C.B., and Simon, M.C. (2002). Phosphatidylinositol 3-kinase/Akt signaling is neither required for hypoxic stabilization of HIF-1 alpha nor sufficient for HIF-1-dependent target gene transcription. J. Biol. Chem. *277*, 15162–15170.

Bindra, R.S., Vasselli, J.R., Stearman, R., Linehan, W.M., and Klausner, R.D. (2002). VHL-mediated hypoxia regulation of cyclin D1 in renal carcinoma cells. Cancer Res. *62*, 3014–3019.

Bonicalzi, M.E., Groulx, I., de Paulsen, N., and Lee, S. (2001). Role of exon 2-encoded beta-domain of the von Hippel-Lindau tumor suppressor protein. J. Biol. Chem. *276*, 1407–1416.

Bruick, R.K. (2000). Expression of the gene encoding the proapoptotic Nip3 protein is induced by hypoxia. Proc. Natl. Acad. Sci. USA *97*, 9082–9087.

Bruick, R.K., and McKnight, S.L. (2001). A conserved family of prolyl-4-hydroxylases that modify HIF. Science *294*, 1337–1340.

Carmeliet, P., Dor, Y., Herbert, J.M., Fukumura, D., Brusselmans, K., Dewerchin, M., Neeman, M., Bono, F., Abramovitch, R., Maxwell, P., et al. (1998). Role of HIF-1alpha in hypoxia-mediated apoptosis, cell proliferation and tumour angiogenesis. Nature *394*, 485–490.

Carrero, P., Okamoto, K., Coumailleau, P., O'Brien, S., Tanaka, H., and Poellinger, L. (2000). Redox-regulated recruitment of the transcriptional coactivators CREB-binding protein and SRC-1 to hypoxia-inducible factor 1alpha. Mol. Cell. Biol. *20*, 402–415.

Cockman, M.E., Masson, N., Mole, D.R., Jaakkola, P., Chang, G.W., Clifford, S.C., Maher, E.R., Pugh, C.W., Ratcliffe, P.J., and Maxwell, P.H. (2000). Hypoxia inducible factor-alpha binding and ubiquitylation by the von Hippel-Lindau tumor suppressor protein. J. Biol. Chem. *275*, 25733–25741.

Di Cristofano, A., Pesce, B., Cordon-Cardo, C., and Pandolfi, P.P. (1998). Pten is essential for embryonic development and tumour suppression. Nat. Genet. *19*, 348–355.

Ebert, B.L., and Bunn, H.F. (1998). Regulation of transcription by hypoxia requires a multiprotein complex that includes hypoxia-inducible factor *1*, an adjacent transcription factor, and p300/CREB binding protein. Mol. Cell. Biol. *18*, 4089–4096.

Epstein, A.C., Gleadle, J.M., McNeill, L.A., Hewitson, K.S., O'Rourke, J., Mole, D.R., Mukherji, M., Metzen, E., Wilson, M.I., Dhanda, A., et al. (2001). C. elegans EGL-9 and mammalian homologs define a family of dioxygenases that regulate HIF by prolyl hydroxylation. Cell *107*, 43–54.

Foster, K., Prowse, A., van den Berg, A., Fleming, S., Hulsbeek, M.M., Crossey, P.A., Richards, F.M., Cairns, P., Affara, N.A., Ferguson-Smith, M.A., et al. (1994). Somatic mutations of the von Hippel-Lindau disease tumour suppressor gene in non-familial clear cell renal carcinoma. Hum. Mol. Genet. *3*, 2169–2173.

Gnarra, J.R., Tory, K., Weng, Y., Schmidt, L., Wei, M.H., Li, H., Latif, F., Liu, S., Chen, F., Duh, F.M., et al. (1994). Mutations of the VHL tumour suppressor gene in renal carcinoma. Nat. Genet. *7*, 85–90.

Gnarra, J.R., Duan, D.R., Weng, Y., Humphrey, J.S., Chen, D.Y., Lee, S., Pause, A., Dudley, C.F., Latif, F., Kuzmin, I., et al. (1996). Molecular cloning of the von Hippel-Lindau tumor suppressor gene and its role in renal carcinoma. Biochim. Biophys. Acta *1242*, 201–210.

Gnarra, J.R., Ward, J.M., Porter, F., Wagner, J., Devor, D., Grinberg, A., Emmert-Buck, M., Westphal, H., Klausner, R.D., and Linehan, W.M. (1997). Defective placental vasculogenesis causes embryonic lethality in VHL-deficient mice. Proc. Natl. Acad. Sci. USA *94*, 9102–9107.

Groulx, I., and Lee, S. (2002). Oxygen-dependent ubiquitination and degradation of hypoxia-inducible factor requires nuclear-cytoplasmic trafficking of the von Hippel-Lindau tumor suppressor protein. Mol. Cell. Biol. *22*, 5319–5336.

Gunawan, B., Huber, W., Holtrup, M., von Heydebreck, A., Efferth, T., Poustka, A., Ringert, R.H., Jakse, G., and Fuzesi, L. (2001). Prognostic impacts of cytogenetic findings in clear cell renal cell carcinoma: gain of 5q31-qter predicts a distinct clinical phenotype with favorable prognosis. Cancer Res. *61*, 7731–7738.

Haase, V.H., Glickman, J.N., Socolovsky, M., and Jaenisch, R. (2001). Vascular tumors in livers with targeted inactivation of the von Hippel-Lindau tumor suppressor. Proc. Natl. Acad. Sci. USA *98*, 1583–1588.

Hanahan, D., and Weinberg, R.A. (2000). The hallmarks of cancer. Cell *100*, 57–70.

Hoffman, M.A., Ohh, M., Yang, H., Klco, J.M., Ivan, M., and Kaelin, W.G., Jr. (2001). von Hippel-Lindau protein mutants linked to type 2C VHL disease preserve the ability to downregulate HIF. Hum. Mol. Genet. *10*, 1019–1027.

Hopfl, G., Wenger, R.H., Ziegler, U., Stallmach, T., Gardelle, O., Achermann, R., Wergin, M., Kaser-Hotz, B., Saunders, H.M., Williams, K.J., et al. (2002). Rescue of hypoxia-inducible factor-1alpha-deficient tumor growth by wild-type cells is independent of vascular endothelial growth factor. Cancer Res. *62*, 2962–2970.

Ikeda, E., Achen, M.G., Breier, G., and Risau, W. (1995). Hypoxia-induced transcriptional activation and increased mRNA stability of vascular endothelial growth factor in C6 glioma cells. J. Biol. Chem. *270*, 19761–19766.

Iliopoulos, O., Kibel, A., Gray, S., and Kaelin, W.G., Jr. (1995). Tumour suppression by the human von Hippel-Lindau gene product. Nat. Med. *1*, 822–826.

Iliopoulos, O., Levy, A.P., Jiang, C., Kaelin, W.G., Jr., and Goldberg, M.A. (1996). Negative regulation of hypoxia-inducible genes by the von Hippel-Lindau protein. Proc. Natl. Acad. Sci. USA *93*, 10595–10599.

Ivan, M., Kondo, K., Yang, H., Kim, W., Valiando, J., Ohh, M., Salic, A., Asara, J.M., Lane, W.S., and Kaelin, W.G., Jr. (2001). HIFalpha targeted for VHL-mediated destruction by proline hydroxylation: implications for O2 sensing. Science *292*, 464–468.

Jaakkola, P., Mole, D.R., Tian, Y.M., Wilson, M.I., Gielbert, J., Gaskell, S.J., Kriegsheim, A.v., Hebestreit, H.F., Mukherji, M., Schofield, C.J., et al. (2001). Targeting of HIF-alpha to the von Hippel-Lindau ubiquitylation complex by O2-regulated prolyl hydroxylation. Science *292*, 468–472.

Jiang, B.H., Zheng, J.Z., Leung, S.W., Roe, P., and Semenza, G.L. (1997). Transactivation and inhibitory domains of hypoxia-inducible factor 1alpha. Modulation of transcriptional activity by oxygen tension. J. Biol. Chem. *272*, 19253–19260.

Kallio, P.J., Wilson, W.J., O'Brien, S., Makino, Y., and Poellinger, L. (1999). Regulation of the hypoxia-inducible transcription factor 1alpha by the ubiquitin-proteasome pathway. J. Biol. Chem. *274*, 6519–6525.

Kamada, M., Suzuki, K., Kato, Y., Okuda, H., and Shuin, T. (2001). von Hippel-Lindau protein promotes the assembly of actin and vinculin and inhibits cell motility. Cancer Res. *61*, 4184–4189.

Kondo, K., Klco, J., Nakamura, E., Lechpammer, M., and Kaelin, W.G., Jr. (2002). Inhibition of HIF is necessary for tumor suppression by the von Hippel-Lindau protein. Cancer Cell *1*, 237–246.

Kozma, L., Kiss, I., Nagy, A., Szakall, S., and Ember, I. (1997). Investigation of c-myc and K-ras amplification in renal clear cell adenocarcinoma. Cancer Lett. *111*, 127–131.

Krieg, M., Haas, R., Brauch, H., Acker, T., Flamme, I., and Plate, K.H. (2000). Up-regulation of hypoxia-inducible factors HIF-1alpha and HIF-2alpha under normoxic conditions in renal carcinoma cells by von Hippel-Lindau tumor suppressor gene loss of function. Oncogene *19*, 5435–5443.

Kung, A.L., Wang, S., Kico, J.M., Kaelin, W.G., Jr., and Livingston, D.M. (2000). Suppression of tumor growth through disruption of hypoxia-inducible transcription. Nat. Med. *6*, 1335–1340.

Lando, D., Peet, D.J., Whelan, D.A., Gorman, J.J., and Whitelaw, M.L. (2002). Asparagine hydroxylation of the HIF transactivation domain a hypoxic switch. Science *295*, 858–861.

Levy, A.P., Levy, N.S., and Goldberg, M.A. (1996a). Post-transcriptional regulation of vascular endothelial growth factor by hypoxia. J. Biol. Chem. *271*, 2746–2753.

Levy, A.P., Levy, N.S., and Goldberg, M.A. (1996b). Hypoxia-inducible protein binding to vascular endothelial growth factor mRNA and its modulation by the von Hippel-Lindau protein. J. Biol. Chem. *271*, 25492–25497.

Liang, Y., Buettger, C., Berner, D.K., and Matschinsky, F.M. (1997). Chronic

effect of fatty acids on insulin release is not through the alteration of glucose metabolism in a pancreatic beta-cell line (beta HC9). Diabetologia *40*, 1018–1027.

Lisztwan, J., Imbert, G., Wirbelauer, C., Gstaiger, M., and Krek, W. (1999). The von Hippel-Lindau tumor suppressor protein is a component of an E3 ubiquitin-protein ligase activity. Genes Dev. *13*, 1822–1833.

Lonergan, K.M., Iliopoulos, O., Ohh, M., Kamura, T., Conway, R.C., Conway, J.W., and Kaelin, W.G., Jr. (1998). Regulation of hypoxia-inducible mRNAs by the von Hippel-Lindau tumor suppressor protein requires binding to complexes containing elongins B/C and Cul2. Mol. Cell. Biol. *18*, 732–741.

Maher, E.R., and Kaelin, W.G., Jr. (1997). von Hippel-Lindau disease. Medicine (Baltimore) *76*, 381–391.

Maltepe, E., Keith, B., Arsham, A.M., Brorson, J.R., and Simon, M.C. (2000). The role of ARNT2 in tumor angiogenesis and the neural response to hypoxia. Biochem. Biophys. Res. Commun. *273*, 231–238.

Maltepe, E., Schmidt, J.V., Baunoch, D., Bradfield, C.A., and Simon, M.C. (1997). Abnormal angiogenesis and responses to glucose and oxygen deprivation in mice lacking the protein ARNT. Nature *386*, 403–407.

Mandriota, S.J., Turner, K.J., Davies, D.R., Murray, P.G., Morgan, N.V., Sowter, H.M., Wykoff, C.C., Maher, E.R., Harris, A.L., Ratcliffe, P.J., and Maxwell, P.H. (2002). HIF activation identifies early lesions in VHL kidneys: evidence for site-specific tumor suppressor function in the nephron. Cancer Cell *1*, 459–468.

Maranchie, J.K., Vasselli, J.R., Riss, J., Bonifacino, J.S., Linehan, W.M., and Klausner, R.D. (2002). The contribution of VHL substrate binding and HIF1-alpha to the phenotype of VHL loss in renal cell carcinoma. Cancer Cell *1*, 247–255.

Maxwell, P.H., Dachs, G.U., Gleadle, J.M., Nicholls, L.G., Harris, A.L., Stratford, I.J., Hakinson, O., Pugh, C.W., and Ratcliffe, P.J. (1997). Hypoxia-inducible factor-1 modulates gene expression in solid tumors and influences both angiogenesis and tumor growth. Proc. Natl. Acad. Sci. USA *94*, 8104–8109.

Maxwell, P.H., Wiesener, M.S., Chang, G.W., Clifford, S.C., Vaux, E.C., Cockman, M.E., Wykoff, C.C., Pugh, C.W., Maher, E.R., and Ratcliffe, P.J. (1999). The tumour suppressor protein VHL targets hypoxia-inducible factors for oxygen-dependent proteolysis. Nature *399*, 271–275.

Mortensen, R.M., Conner, D.A., Chao, S., Geisterfer-Lowrance, A., and Seidman, J. (1992). Production of homozygous mutant ES cells with a single targeting construct. Mol. Cell. Biol. *12*, 2391–2395.

Ohh, M., Yauch, R.L., Lonergan, K.M., Whaley, J.M., Stemmer-Rachamimov, A.O., Louis, D.N., Gavin, B.J., Kley, N., Kaelin, W.G., Jr., and Iliopoulos, O. (1998). The von Hippel-Lindau tumor suppressor protein is required for proper assembly of an extracellular fibronectin matrix. Mol. Cell *1*, 959–968.

Ohh, M., Park, C.W., Ivan, M., Hoffman, M.A., Kim, T.Y., Huang, L.E., Pavletich, N. Chau, V., and Kaelin, W.G., Jr. (2000). Ubiquitination of hypoxia-inducible factor requires direct binding to the beta-domain of the von Hippel-Lindau protein. Nat. Cell Biol. *2*, 423–427.

Pause, A., Lee, S., Worrell, R.A., Chen, D.Y., Burgess, W.H., Linehan, W.M., and Klausner, R.D. (1997). The von Hippel-Lindau tumor-suppressor gene product forms a stable complex with human CUL-2, a member of the Cdc53 family of proteins. Proc. Natl. Acad. Sci. USA *94*, 2156–2161.

Pause, A., Lee, S., Lonergan, K.M., and Klausner, R.D. (1998). The von Hippel-Lindau tumor suppressor gene is required for cell cycle exit upon serum withdrawal. Proc. Natl. Acad. Sci. USA *95*, 993–998.

Pugh, C.W., O'Rourke, J.F., Nagao, M., Gleadle, J.M., and Ratcliffe, P.J. (1997). Activation of hypoxia-inducible factor-1; definition of regulatory domains within the alpha subunit. J. Biol. Chem. *272*, 11205–11214.

Reiter, R.E., Anglard, P., Liu, S., Gnarra, J.R., and Linehan, W.M. (1993). Chromosome 17p deletions and p53 mutations in renal cell carcinoma. Cancer Res. *53*, 3092–3097.

Ryan, H.E., Lo, J., and Johnson, R.S. (1998). HIF-1a is required for solid tumor formation and embryonic vascularization. EMBO J. *17*, 3005–3015.

Ryan, H.E., Poloni, M., McNulty, W., Elson, D., Gassmann, M., Arbeit, J.M., and Johnson, R.S. (2000). Hypoxia-inducible factor-1alpha is a positive factor in solid tumor growth. Cancer Res. *60*, 4010–4015.

Sang, N., Fang, J., Srinivas, V., Leshchinsky, I., and Caro, J. (2002). Carboxyl-terminal transactivation activity of hypoxia-inducible factor 1 alpha is governed by a von Hippel-Lindau protein-independent, hydroxylation-regulated association with p300/CBP. Mol. Cell. Biol. *22*, 2984–2992.

Sowter, H.M., Ratcliffe, P.J., Watson, P., Greenberg, A.H., and Harris, A.L. (2001). HIF-1-dependent regulation of hypoxic induction of the cell death factors BNIP3 and NIX in human tumors. Cancer Res. *61*, 6669–6673.

Stiles, B., Gilman, V., Khanzenson, N., Lesche, R., Li, A., Qiao, R., Liu, X., and Wu, H. (2002). Essential role of AKT-1/protein kinase B alpha in PTEN-controlled tumorigenesis. Mol. Cell. Biol. *22*, 3842–3851.

Tanimoto, K., Makino, Y., Pereira, T., and Poellinger, L. (2000). Mechanism of regulation of the hypoxia-inducible factor-1 alpha by the von Hippel-Lindau tumor suppressor protein. EMBO J. *19*, 4298–4309.

Turner, K.J., Moore, J.W., Jones, A., Taylor, C.F., Cuthbert-Heavens, D., Han, C., Leek, R.D., Gatter, K.C., Maxwell, P.H., Ratcliffe, P.J., et al. (2002). Expression of hypoxia-inducible factors in human renal cancer: relationship to angiogenesis and to the von Hippel-Lindau gene mutation. Cancer Res. *62*, 2957–2961.